S. Afr. J. Chem., 2025, 79, 142–151
https://journals.co.za/content/journal/chem/

Chemical Speciation of Copper(II) 1,4-Diazepane Derivative of Pentacyclodecane: A Potential Anti-inflammatory Agent

Graham E. Jackson[1,2*], Kagiso Mokalane[1†], Hendrik G. Kruger[3], Oluseye K. Onajole[3,4], Ahmed N. Hammouda[1,5] & Fatin M. Elmagbari[1,5]

[1]*Department of Chemistry, University of Cape Town, Rondebosch, South Africa.*
[2]*Department of Chemistry, University of Melbourne, Victoria, Australia.*
[3]*School of Chemistry, University of KwaZulu-Natal, Durban, South Africa.*
[4]*Department of Biological, Physical and Health Sciences, Roosevelt University, Chicago, IL, USA.*
[5]*Department of Chemistry, Faculty of Science, University of Benghazi, Benghazi, Libya.*

ABSTRACT

Formation constants of copper(II) with 1,1′-(8,11-oxapentacyclo[5.4.0.0^{2,6}.0^{3,10}.0^{5,9}]undec-8,11-diethylene)-bis(1,4-diazepane) (L^1) and 1,4-diazepane (L^2) have been studied by glass electrode potentiometry at 25 °C and an ionic strength of 0.15 mol dm^{-3}. UV/Vis spectroscopy, NMR spectroscopy and molecular mechanics results suggest that the Cu(II) is coordinated to both diazepane derivatives on pentacyclodecane in a distorted tetragonal geometry. Speciation calculations of Cu(II) using a blood plasma model indicated that L^1 is not good at mobilising copper *in vivo*, even at high ligand concentrations. Tissue permeability studies were performed using a modified Franz cell and a Cerasome 9005 membrane, where K_p (permeability coefficient) was found to be 5.06×10^{-6} cm/s (± 0.03). These results suggest that L^1 is unlikely to significantly improve the dermal absorption of copper(II).

KEYWORDS

copper speciation, glass electrode potentiometry, anti inflammatory, equilibrium constants, tissue permeability

Received 23 August 2024, revised 26 August 2025, accepted 2 September 2025

INTRODUCTION

Rheumatoid arthritis (RA) is a chronic, systemic inflammatory disorder principally affecting synovial tissues.[1] It is an autoimmune disease, although the exact cause is still unknown.[2,3–6] The disease occurs first in the knuckle joints and chiefly affects the joint synovial membranes.[7,8] The disease is managed with immunosuppressive drugs, and its symptoms are treated with anti-inflammatory drugs, the goal being to control joint inflammation and prevent joint damage and disability. The medicinal properties of copper have long been known;[9] however, Sorenson[10] renewed interest in the anti-inflammatory effects of copper when he found that the active forms of anti-inflammatory drugs are their Cu-complexes *in vivo.* Copper bangles have been used to suppress the inflammation associated with RA,[10–12] and Walker and Keats[12] have measured significant dermal absorption of copper from these bracelets. Because of the circumstantial evidence surrounding the use of copper (II) in the treatment of inflammatory diseases, we and others have tried to design ligands which will increase the bioavailability of copper (II) *in vivo*. The ligand should be primarily a nitrogen donor ligand so that the selectivity for copper is increased without disrupting the homeostasis of other metal ions *in vivo*. The complex should also be kinetically labile, so that the copper ion is released at the site of inflammation. Furthermore, the resultant copper (II) complex should be lipophilic to facilitate dermal absorption.[13–15]

Jackson *et al.* have investigated the solution chemistry of Cu(II), Ca(II), and Zn(II) with 3,5-diaminodiamido-4-oxahexacyclododecane (cage-L, Figure 1) as a potential anti-inflammatory drug.[7] The chemistry of pentacycloundecane cage derivatives has been extensively studied, and several amino cage compounds with promising pharmaceutical activities have been found.[5,16] The large lipophilic nature of the cage moiety facilitates the passage through membranes. Potentiometric results showed that cage-L forms stable complexes with Cu(II), but blood plasma simulation studies predicted that the ligand was not able to mobilise Cu(II) *in vivo*, because of interference from Zn(II) and Ca(II). The results from partition coefficient experiments suggested that the copper (II) complex of cage-L was largely hydrophilic, but that at least 2.9% of the complex was extracted into the organic phase. Biodistribution studies, using ^{64}Cu-labelled Cu(II)-cage-L, revealed that ~50% of the copper was still retained in the body 24 hrs after injection.[2]

The reason for the poor *in vivo* mobilisation of copper by cage-L was the presence of two amides in the ligand. While these were designed to increase the lipophilicity of the copper complex, they also decreased the stability of the complex. For this reason, in this study, we have used an amine analogue of cage-L, 1,1'-(8,11-oxapentacyclo[5.4.0.0^{2,6}.0^{3,10}.0^{5,9}]undec-8,11-diethylene)-bis(1,4-diazepane) (L^1) (Figure 1), where two alkene bridges have linked the two nitrogen donor groups, making 1,4-diazepane (L^2).

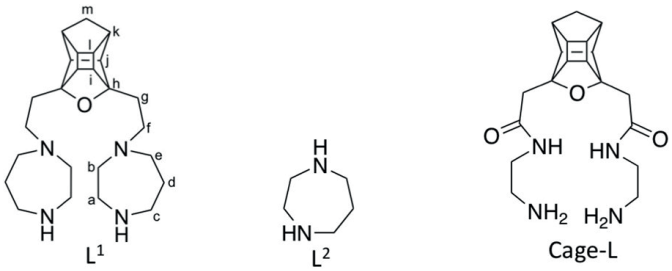

Figure 1: Structures of (1,1′-(8,11-oxapentacyclo[5.4.0.0^{2,6}.0^{3,10}.0^{5,9}]undec-8,11-diethylene)-bis(1,4-diazepane)) L^1 and (1,4-diazepane) L^2 investigated in this study and related ligand (8,11-oxapentacyclo[5.4.0.0^{2,6}.0^{3,10}.0^{5,9}]undec-8,11-diacetylcarboxamido-bis(ethylamine) cage-L

*To whom correspondence should be addressed
Email: graham.jackson@uct.ac.za
†This paper is dedicated to Kagiso Mokalane, who passed away before it could be published.

ISSN 1996-840X Online / South African Chemical Institute / http://saci.co.za/journal

https://doi.org/10.17159/0379-4350/2025/v79a15

EXPERIMENTAL

Equipment

The NMR spectroscopy data of L^1 were recorded on a Bruker AVANCE III 400 MHz instrument using $CDCl_3$ as a solvent. All chemical shifts (δ) are quoted in parts per million downfield from TMS, and the coupling constants (*J*) are recorded in Hertz. Splitting pattern abbreviations are: s = singlet, d = doublet, t = triplet, m = multiplet, br = broad. Infrared spectra were obtained on a Perkin Elmer Spectrum 100 instrument with an Attenuated Total Reflectance attachment, recorded in cm^{-1}. All reactions were monitored using Thin Layer Chromatography (TLC, Merck Kieselgel 60, F254). All purifications were carried out by Column Chromatography using Fluka Kieselgel 60 (70 – 230 mesh) with CH_3Cl:CH_3OH:NH_4OH (88:10:2) as the eluent (solvent mixture). The level of purity for all compounds was judged to be >95% based on ^1H NMR and LC-MS analysis. Mass Spectra were obtained using a Waters LCT Premier Time of Flight mass spectrometer. Tetrahydrofuran was freshly distilled before use from sodium benzophenone under N_2 atmosphere, while dichloromethane was dried using phosphorus pentoxide. The syntheses of the precursors are described in their corresponding references.

Synthesis of L^1

To a vigorously stirred solution of the 1,4-diazepane (22 mmol) in CH_2Cl_2 (400 mL) at -78 °C (dry ice, 2-propanol) under a N_2 atmosphere, a solution of (hexahydro-2*H*-2,6,3,5-(epiethane[1,1,2,2] tetrayl)pentaleno[1,6-*bc*]furan-2,6a(2a*H*)-diyl)bis(ethane-2,1-diyl) bis(4-methylbenzenesulfonate) (1.2 g, 2.2 mmol) in CH_2Cl_2 (100 mL), was added dropwise over 45 minutes. The reaction mixture was left to attain room temperature with stirring for 24 hours. The solution was washed with water to remove excess diamines; the obtained organic extract was dried over Na_2SO_4 and concentrated *in vacuo*. The crude residue was purified *via* column chromatography using $CHCl_3$: MeOH: NH_4OH (88:10:2) to obtain L^1 as a pure light-yellow oil (R_f = 0.2, 0.55 g, 62 %). IR ν_{max}: broad absorption (N-H) 3386, 2818, 1465, 1108, 927, 918 and 748 cm^{-1}. HRMS calculated for $C_{25}H_{40}N_4O$ (M + H^+) 413.3280 found 413.3287. ^1H NMR [$CDCl_3$, 400 MHz] δ_H 1.48 (*AB*, J_{AB} = 10.2 Hz, 1H; H_m), 1.84 (AB, J_{AB} = 10.2 Hz, 1H; H_m), 1.76 (2H; H_d), 1.98 (2H; H_g), 2.35-2.69 (m, 10H; H_b, H_e, H_f, H_i - H_l), 2.89-2.94 (m, 4H; H_c and H_a). ^{13}C NMR [$CDCl_3$, 100 MHz]: δ_C 30.0 (t; C_d), 30.4 (t: C_g), 41.8 (d: C_l), 43.4 (t: C_m), 44.5 (d: C_k), 47.2 (t: C_c), 48.0 (d: C_i), 48.6 (d: C_a), 54.5-54.6 (t: C_e and C_d), 57.8 (t: C_b), 58.8 (d: C_j), 94.8 (s: C_h). For atom labelling, refer to Figure 1.

Potentiometry Titration

All titrations were carried out in an inert atmosphere of purified nitrogen using a Metrohm Titrino 799 equipped with a combined glass electrode (Metrohm 6.0222.100) calibrated in terms of hydrogen ion concentration before each titration. The electrode slope was determined *in situ*. All solutions were prepared in MiliQ water, which was boiled to remove any dissolved CO_2. Double glass boiled distilled water with recrystallised NaCl (Fluka) was used as the background electrolyte, at an ionic strength of 0.15 mol dm^{-3} (Cl^-) Na^+. Other reagents, copper (II) chloride dehydrate, zinc (II) chloride, calcium (II) chloride dehydrate, and EDTA (Merk) were commercially available and of analytical grade. The 0.1 mol dm^{-3} solutions of NaOH and HCl were prepared from Merck Titrisol ampoules and standardised by titrating with potassium hydrogen phthalate (KHP) and sodium tetraborate decahydrate (Borax), respectively, using standard methods of Vogel.[17] The NaOH solutions prepared were further standardised against the standard HCl solution. Potentiometric titrations were carried out in the pH range 2-11, with the Cu(II) concentration in the range 0.001-0.00087 mol dm^{-3}, and metal-to-ligand ratios of 1:2, 1:3, and 1:4 for each ligand system. Under these conditions, the water ionisation constant was determined to be between 13.8 and 13.6 log units. Equilibrium constants were evaluated from the potentiometric titration data using the ESTA suite of computer programs using a procedure described previously.[18]

UV/Visible and Nuclear Magnetic Resonance Spectroscopy

Samples for visible spectroscopy (*d–d* transitions) studies were prepared in H_2O at a metal:ligand ratio of 1:2 and concentration of Cu(II) ion ($CuCl_2$) as 0.001 – 0.00085 M. UV/Vis spectra were recorded in the wavelength region between 340 and 800 nm at 25 °C in 1.00 cm quartz cells using a Hewlett Packard 8425A Diode Array spectrometer equipped with a temperature controlled cell holder. Spectra were recorded over the pH range 2-9 due to difficulties with the formation of a precipitate at higher pH values. Small amounts of 0.1 M NaOH and HCl were used to adjust the pH during the titration.

NMR spectra were recorded on a Varian Unity Plus 400 MHz instrument. NMR samples were prepared in D_2O solution at the same metal-to-ligand ratios as used for the UV/Vis spectroscopy studies, and the pH of the solution was adjusted using NaOD or DCl. The pH of the solution was corrected for the deuterium isotope effect using:

$$pH = 0.929pD + 0.41 \quad (1)$$

where, pH is a direct reading in D_2O solution of the H_2O-calibrated pH meter.

Bio-modelling measurements

Blood plasma modelling was performed using the ECCLES database, into which the constants determined in this study had been incorporated.[19] Plasma mobilising index (PMI) is defined as the ability of a specific ligand to increase the low molecular weight (l.m.w.) concentration of a specific metal ion *in vivo*. The blood plasma database consists of seven metal ions, forty ligands, and 250 published mononuclear binary constants, measured under physiological conditions, with another 400 measured under non-physiological conditions and 100 ternary complex constants. The plasma mobilising index (PMI) was calculated according to the expression:

$$PMI = C_1 / C_2 \quad (2)$$

where, C_1 is the total concentration of l.m.w. metal ion complexes in the presence of the drug and C_2 is the total concentration of l.m.w. metal ion complexes in normal plasma.

Molecular mechanics

Molecular mechanics calculations were performed on a SyncMaster 1100 p workstation using the Discover 3 module of Insight II software.[20] The extensible systematic force field (esff) was used for all energy calculations.

Franz diffusion cells

A stock solution CuL^1 was prepared by mixing 10 mL of 0.01 mol dm^{-3} copper (II) chloride solution and 20 mL of 0.076 mol dm^{-3} L^1 solution. The pH of the solution was then raised to 7.2 by adding small amounts of NaOH solution. In this study, the Franz cell was used with a synthetic membrane, which was used to mimic the human skin. The lipid membrane was prepared by soaking trimmed circular discs of Whatman filter paper in a Cerasome 9005 (purchased from Lipoid GmbH, Germany) solution for 3 hours and air-drying with tweezers. Each membrane was weighed before being used in the experiment.

The permeation coefficient, K_p, is the ratio of the steady-state flux (*J*) of the drug across the membrane and the applied dose:

$$K_p = J / Ci \quad (3)$$

where J is the number of mg/cm^2. h of the permeant crossing the membrane, and Ci is the concentration of the drug in the donor phase. The steady-state flux, J, can be expressed as:

$$J = Q / A.t \quad (4)$$

where Q (mg) is the quantity of drug diffusing through the membrane of area A (cm^2) in time t (hrs). In our case, the drug is copper, and so Ci and Q are the concentration and amount of Cu(II).

RESULTS AND DISCUSSION

Potentiometry

Potentiometric results for L^1 and L^2 are presented in Table 1. pK_1 of 1,4-diazepane (L^2) is 0.77 log units greater than that of a related derivative, piperazine (pK_1 9.44). The positive inductive effect of the extra methylene group in L^2 causes this. A similar increase in base strength, brought about by alkyl substitution, is shown by the series: N,N'dimethylethylenediamine (pK_{a1}, 10.17), N,N'-diethylethylenediamine (pK_{a1}, 10.46) and N,N'dipropylenediamine (10.97). The pK_{a1} of 1,4-diazepane is 0.36 log units less than that of methylamine (10.64).[21] This is expected in moving from primary to secondary amines, where steric hindrance and solvation effects are reported to override the positive inductive effects.[21,22]

The relatively low pK_{a2} value (9.11) for the second protonation site of L^2 compared to the first (pK_{a1}), even though the two are symmetry-related, is due to the coulombic repulsion between the incoming proton and the proton already attached to the ligand.[23] Statistical factors must also play a role as the stability constants decrease with decreasing number of available binding sites on the ligand.[24,25]

In L^1, the amines are no longer equivalent, one being a secondary amine and the other a tertiary amine. Hence, there are two possibilities for pK_{a1}, protonation at the secondary or tertiary amine. From the pK_a of dimethylamine and trimethylamine, it is tempting to conclude that it is the secondary amine that is being protonated. Without spectroscopic evidence, however, this conclusion can only be tentative. The small difference, of 1.17 log units, observed between the first and second protonation constants indicates that the second proton is added to the other 1,4-diazepane substituent.

Metal complex formation curves were obtained at 2:1 to 3:1 ligand to metal ratios with the metal ion concentrations in the range 0.01-0.0087 mol.dm^{-3}. The complex formation, Z_M-bar (eqn 5), function was used to visualise the experimental data and to decide on the speciation model for Cu(II) complexation. Z_M-bar measures the number of ligands bound per metal. The classical Z_M-bar function is strictly only defined for simple mononuclear complex formation, but deviation from ideal behaviour is indicative of the different speciation occurring in solution. Thus, if, as in this case, the Z_M-bar curves fan back, hydroxyl species formation is indicated. If the curves at different metal-to-ligand ratios are not superimposable, protonated and/or polynuclear complex species are indicated.

$$Z_M = (T_L - [L]) / T_M \quad (5)$$

where T_L and T_M are the total concentration of the ligand, proton, and metal, respectively, and [L] is the free-ligand concentration.

The Z_M-bar function for the Cu(II)–L^1 system is plotted against pL (–log[L]) in Figure 2a. Between pL values of 15 to 10, the formation curves rise and level off at ~ 0.6 before continuing to rise to a value of 1. The curve levelling off at 1 suggests the formation of a 1:1 M:L species, but the levelling off at 0.6 indicates that, at low pH, this is not the only metal species present in the solution. A Z_M-bar value of 0.5 suggests a species with the M:L ratio of 2:1. At pL values < 10, the Z_M-bar curve increases and fans back, indicating the formation of hydroxy species. The curves at different M:L ratios are not superimposable because the formation of the hydroxy species occurs at different pH values, depending on the M:L ratio. The Z_M-bar function is not sensitive to the formation of protonated species, so it is difficult to distinguish between ML and MLH.

Table 1: Logarithms of the overall stability constant, logβ_{pqr} for $M_pL_qH_r$ complexes of H^+ and Cu^{+2} with L^1 and L^2 determined at 25 °C and I = 0.15 mol dm^{-3} (Cl^-)Na^+ in the pH range 2-11. δ_{pqr} denotes the standard deviation in logβ_{pqr}, R^H is the Hamiltonian R-factor and $R_{lim}{}^H$ its limit. n_T and n_P are the number of titrations and points, respectively.

Ligand	p q r	Logβ_{pqr}	δ_{pqr}	R^H	$R_{lim}{}^H$	$n_T(n_p)$
H^+- L^1	0 1 1	10.28	0.01	0.006	0.01	2(162)
	0 1 2	19.39	0.01			
	0 1 3	26.27	0.01			
	0 1 4	31.71	0.02			
Cu^{+2}- L^1	2 1 1	21.22	0.03	0.02	0.02	2(180)
	1 1 1	17.60	0.03			
	1 1 0	09.25	0.02			
	1 1 -1	-1.39	0.03			
[a]H^+-L^2	0 1 1	10.21	0.002	0.01	0.008	2(136)
	0 1 2	17.09	0.003			
[a]Cu^{+2}-L^2	1 1 0	7.6	0.01	0.03	0.02	3(600)
	1 2 0	12.6	0.01			
	1 1 -1	1.88	0.03			

[a]The values for L^2 are in close agreement with literature values, given the difference in ionic strength and temperature.[26]

The Z_M-bar curves for L^2 (Figure 2c) are similar to those of L^1 but are displaced to much lower pL values, indicating that the L^2 complexes are not as stable as the L^1 complexes. Also, at high M:L ratios, the Z_M-bar curves tend towards a value of 2 before fanning back, indicating the formation of ML_2. Since L^2 is a bidentate ligand, two ligands can coordinate with the metal ion.

The potentiometric data were analysed using the ESTA suite of computer programs, which yielded the results in Table 1. The low standard deviation in the logβ_{pqr}'s, the low Hamilton R factors, and the agreement between the observed and calculated data for Z_M-bar lends confidence to the results. From potentiometric data alone, it is impossible to tell the structure of the different complexes formed. However, by comparison with known systems, it is possible to make some inferences as to the site of coordination. From the species distribution curve in Figure 2(b), calculated from the data for L^1 in Table 1, complexation starts at pH 2.0 with the formation of M_2LH, which reaches a maximum at pH ~3, when MLH starts to form. It is possible that the Cu(II) binds to only one nitrogen of L^2, but if we consider the equilibrium M + LH = MLH, the equilibrium constant is calculated to be 7.3 (logβ_{111} – logβ_{011}), which is too high for monodentate coordination. In fact, this value is very close to the equilibrium constant (logβ_{110} 7.6) for ML of L^2, which is a bidentate ligand. Also, if we consider M_2LH to be formed from the coordination of a second metal ion to MLH, the equilibrium constant (logβ_{211} – logβ_{111}) is 3.62. This is very close to the value of logβ_{110} (4.11) of Cu/methylamine.

L^2 is a bidentate ligand, which is reflected in the log β_{110} of 7.6. The log β_{110} of L^1 is higher at 9.25. Given the similar basicity of L^1 and L^2, one would expect similar values for log β_{110}. Thus, L^1 must be operating as a tetradentate ligand. This would explain the existence of the MLH species of L^1, where one of the nitrogens is protonated. This species was not found for L^2 since both nitrogens coordinate with Cu(II). This is also why there is no ML_2 species for L^1.

The pKa of the ML species (logβ_{110} – log$\beta_{11\text{-}1}$) is 10.6 and 9.5 for L^1 and L^2, respectively. These values are comparable to the Cu(II) hydrolysis constants, and so it is suggested that the proton is lost from a coordinated water molecule. The species distribution curve for L^2 is shown in Figure 2d.

The ligand cage-L, was found not to mobilise copper *in vivo* because of its binding to Zn(II) and Ca(II).[6] For this reason, attempts were

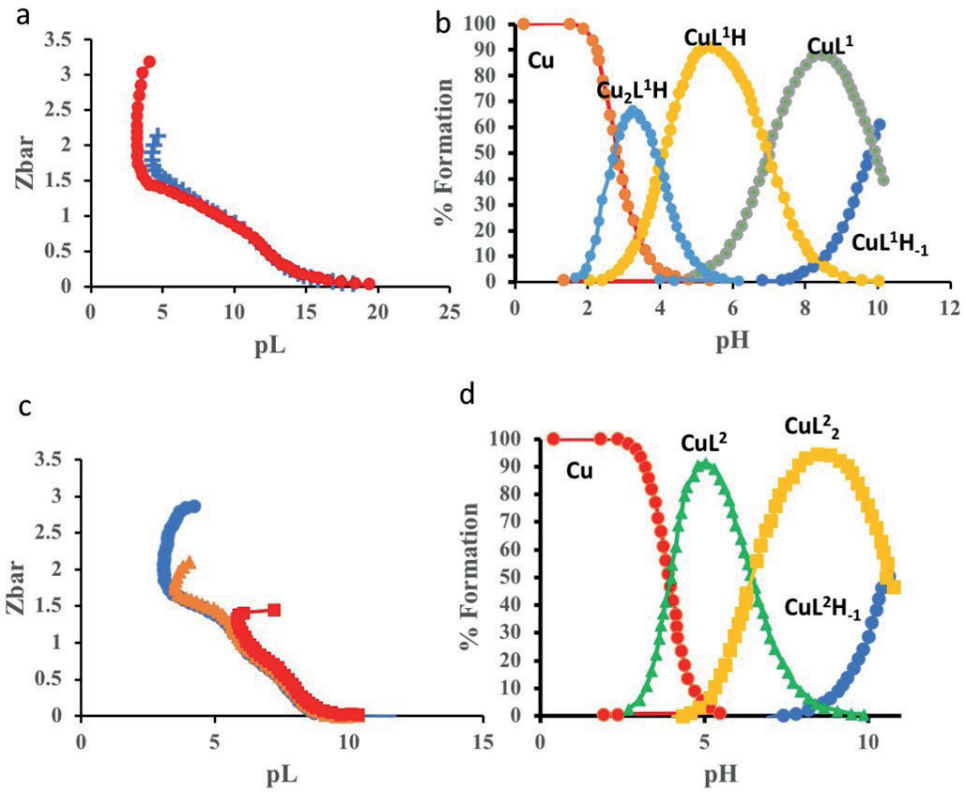

Figure 2: Formation function curve, Z_M-bar against pL for the (a) Cu(II)-(L^1) and (b) Cu(II)-(L^2) systems. Copper species percentage distribution curves of L^1(c) & L^2(d) (1:2 M:L ratios) as a function of pH. The symbols represent complexation curves for various metals to ligand ratios, 1:3 and 1:2, while the solid theoretical line was calculated using the model in Table 1.

made to measure the binding constants of L^1 with these two metal ions. However, no Zn(II) or Ca(II) complexes were detected in the pH range 2-11. Pagano *et al.* could also not detect any complexation between Zn(II) and L^2.[26]

NMR Spectroscopy

NMR spectroscopy was used to determine the sequence of protonation on L^1 and to gain some insights into where the metal coordinates to these ligands. Figure 3(b) shows plots of changes in proton chemical shifts, as a function of pH, where **a**, **c** and **b**, **e**, **f** refer to the chemical shift of the protons attached to carbons next to the secondary and tertiary amine groups, respectively. From the potentiometry results, it was agrued that the first site of protonation was the tertiary amines and then the secondary amines. Form the NMR results, however, a more complicated protonation sequence is suggested. Between pH 1 – 4 (Figure 3(a)), none of the proton signals shift indicating that no protonation is taking place. Between pH 4 – 6, the ^{1}H signals of all the protons shift upfield, but peaks labelled **b**, **e**, and **f** are shifted significantly more upfield. This suggests that, in this pH range, a tertiary amine is being protonated. From the change in chemical shift plot (Figure 3b), the micro-protonation constant of the tertiary amine is estimated to be 5.6, which is close to pK_{a4} obtained from potentiometry. Looking at proton **c**, this has an inflection point at ~pH 6, suggesting that a secondary amine is being protonated. This corresponds to pK_{a3}. Between pH 8 and 10 all the protons shift upfield, which corresponds to pK_{a1} and pK_{a2}. Remembering that the two tertiary and two secondary amines are equivalent, and that there would be rapid proton transfer between them, the protonation sequence in Figure 4 is suggested.

The ^{1}H NMR spectra of the Cu(II)-L^1 system, as a function of Cu(II) concentration, are shown in Figure 5. Cu(II) is paramagnetic, which can affect both the chemical shift and relaxation time of the protons.[27,28] This manifests itself in a broadening and shifting of the NMR signals. The broadening effect of the metal is attenuated by $1/r^6$, where r is the internuclear distance between the Cu(II) and the observed proton.[2] Cu(II) exchange is very rapid on the NMR time scale, and so only an average spectrum is seen for the free and bound ligand.[6]

At pH 7, the signals of **a**, **c**, and **d** broaden significantly with the addition of copper. The rest of the signals remain almost unchanged. This result suggests that only the secondary amines (either one or both) coordinate to the central metal ion. From potentiometry, at this pH, the CuLH species predominates. At pH 8 (Figure 5(a)), all the protons attached to carbons close to the amine groups (**a**, **b**, **c**, **d**, **e**, and **f**) broaden. Signals **a**, **c**, and **f** almost disappear as the concentration of the metal is increased further. These observations suggest that the metal ion is coordinated with all the amine nitrogen atoms. In this pH region, the CuL species predominates. However, from close inspection of the ^{1}H spectrum, signals **b** and **e** do not broaden and shift to the same extent as the other signals, thus suggesting that the coordination geometry of CuL, involves two secondary amines (i.e., the terminal amines) and one tertiary amine being coordinated to copper (II) with the other tertiary amine uncoordinated. Rapid interconversion between different coordination isomers would then lead to the observed broadening. This is consistent with the result from potentiometry.

UV/Visible spectroscopy

Since Cu(II) is a d^9 system, its crystal-field splitting energy is affected by the coordination sphere around it and, hence, the observed λ_{max} affords a measure of the structure of the complexes formed in solution.[29] Distinct colour changes were noted during the potentiometric titrations of the Cu(II)–L^1 system. This is because the solution speciation changes with pH, and the different species formed in the solution have different absorption spectra. The aqueous electronic spectra of the Cu-L^1 system, as a function of pH, are shown in Figure 6. To gain more insight into the coordination geometries of the different complexes present, the spectra of individual species were calculated from the UV/Vis spectroscopy data. This was done using

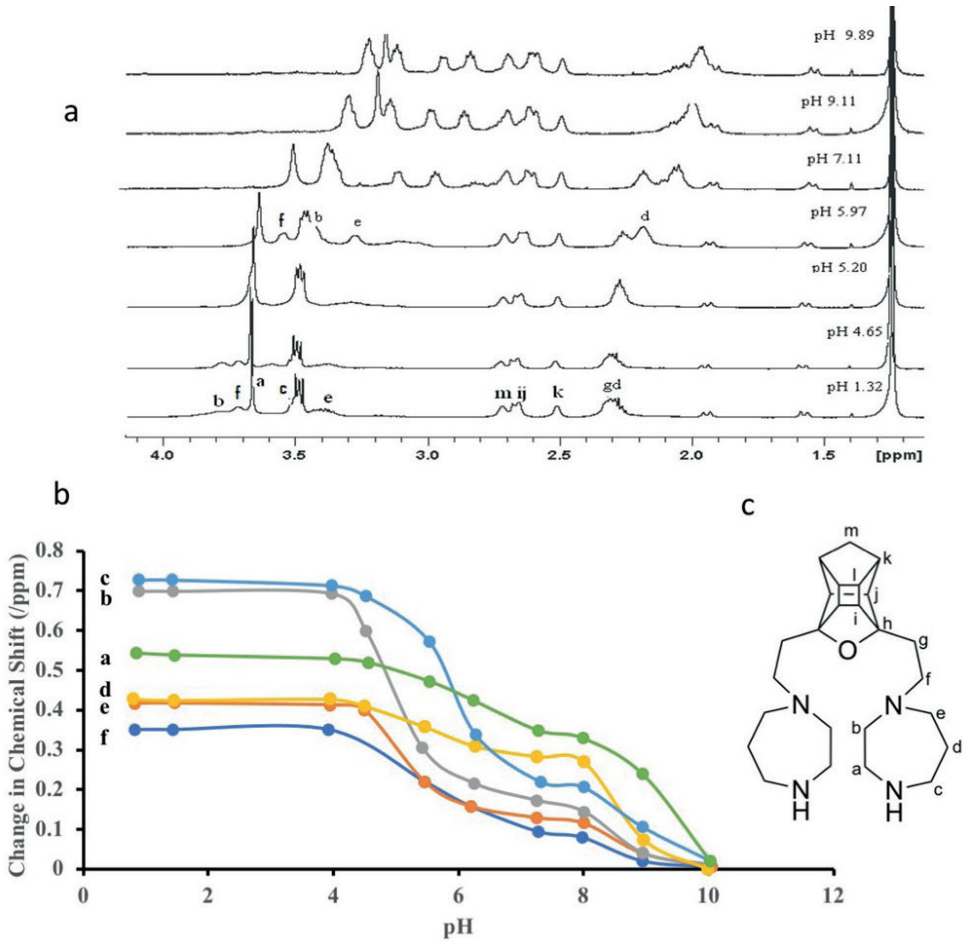

Figure 3: (a) ^{1}H NMR spectra of L^1 as a function of pH. (b) Change in proton chemical shift (ppm) as a function of pH for L^1. (c) The structural formula of L^1 showing atom labelling.

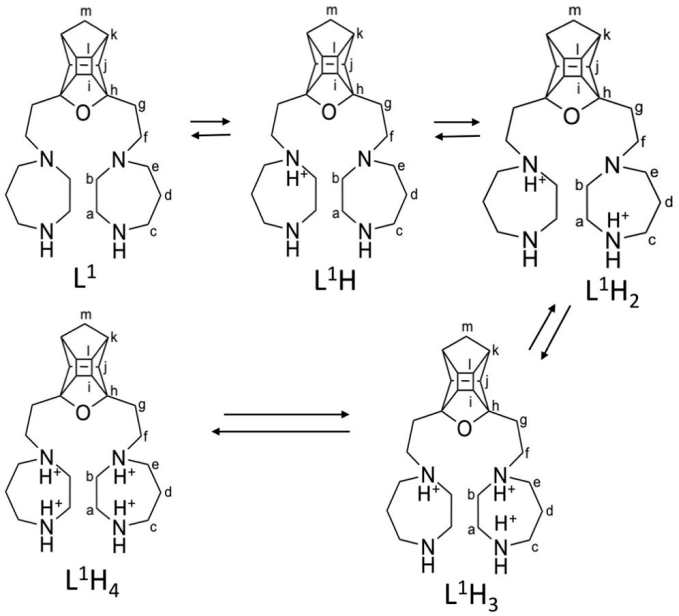

Figure 4: Possible protonation scheme for L^1.

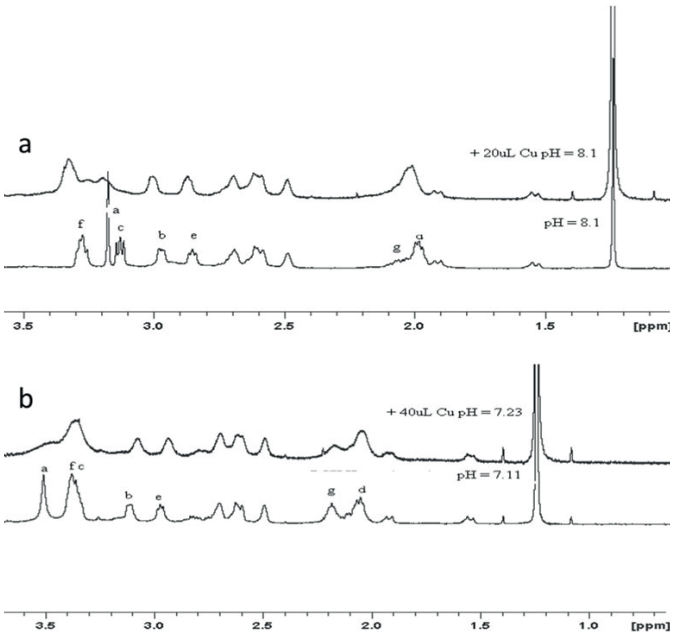

Figure 5: ^{1}H NMR spectra for complexation of Cu(II) with L^1 as a function of copper (II) concentration. (a) 20 µL $Cu(II)Cl_2$, pH 8.1, (b) 40 µL $Cu(II)Cl_2$, pH 7.23. The proton assignments are according to Figure 3(c).

a local program to solve the expanded Beer-Lambert Law equation based on the potentiometric model.[31,32] Upon deconvolution, a single broad absorption band was observed for each species, which enveloped the expected three spin-allowed transitions of a tetragonally distorted Cu(II) complex: $^{2}A_{1g} \leftarrow {}^{2}B_{1g}$, $^{2}B_{2g} \leftarrow {}^{2}B_{1g}$, and $^{2}E_{g} \leftarrow {}^{2}B_{1g}$.[30]

In Figure 6, at pH 4.4, a broad absorption band with an absorption maximum of ~670 nm, indicates that complexation has already started with the formation of M_2LH. As the pH of the solution is increased, the absorbance of the solution increases and shifts to a shorter wavelength. This is caused by the coordination of the amine groups to the Cu(II) ion. At pH 5.3, the CuL^1H species predominates, and the

absorption maximum of 642 nm and a molar extinction coefficient (ε) of 55.63 $dm^3.mol^{-1}.cm^{-1}$ can be assigned to this species. At a pH of 8.3, the ML species predominates, and the absorption maximum of 614 nm (57 $dm^3.mol^{-1}.cm^{-1}$) is assigned to this species. A further increase in the solution pH to 10 causes very little change in the absorption spectrum, but an absorption maximum of 606 nm (ε = 74 $dm^3.mol^{-1}.cm^{-1}$) can be estimated for the MLH_{-1} species. This extra intensity of the absorption band is caused by increased distortion of the metal coordination geometry resulting from ionisation of an axially coordinated water molecule.[31]

Billo has developed a simple empirical method, which can be used to calculate the total electronic transition energy contribution from donor atoms in the coordination sphere of Cu(II).[31] This is given by the following:

$$\nu_{calc} = \Sigma\nu_i \quad (6)$$

where, ν_i is the energy contribution of each donor atom (amide 4.85 ± 0.04 x 10^3; amine 4.53 ± 0.07 x 10^3; carbonyl, OH^-, H_2O 3.01 ± 0.03 x 10^3; carboxylate 3.42 ± 0.10 x 10^3; oxime nitrogen 3.38 x 10^3; cm^{-1}), and the summation is over all the donor atoms.

Figure 7 shows various possible structures for the different species, together with their theoretical λ_{max}, calculated using Billo's method.[31] Since M_2LH has two metal ions, there should be two absorption bands, but because they are very broad, only a single absorption band would be seen. The assigned λ_{max} (670 nm) is between the two λ_{max} values calculated for the two copper ions (737 nm and 663 nm) in Figure 7a. The observed λ_{max} for CuLH (642 nm) is some 21 nm lower than the theoretical value calculated for two amines bound to the central metal ion (structure 7b) but is 41 nm higher than the theoretical value for 3xN coordination. Since Billo's method only looks at equatorial coordination, it is possible that there is some axial N coordination. The CuL species is observed to have a λ_{max} of 614 nm (ε = 74 $dm^3.mol^{-1}.cm^{-1}$), which is close to the value of 602 nm predicted by Billo's method for structures 6(c) and is characteristic of equatorial coordination of amines.[32] However, this value is less than the λ_{max} of $[Cu(II)(NH_3)_3(H_2O)_3]$, which is 645 nm.[30] A similar observation was noted by Linder *et al.* for the tridentate complex of N, N-bis[2-(diethylamino)ethyl]-ethanediamine.[33] This conclusion is consistent with the assumption from potentiometry, which states that the CuL species is formed by the coordination of three amine groups to the central metal ion.

From pH 9 to 10, ML deprotonates to form MLH_{-1} (λ_{max} = 606 nm), which is also consistent with structure 7c. This is consistent with the conclusion from potentiometry, where it is postulated that it is a coordinated water molecule that is deprotonating, since coordinated OH^- and H_2O have the same ligand field effect.

Molecular Mechanics studies

Molecular mechanics (MM) has been used extensively to gain insight into the energy involved in forming different organic compounds.[34] However, its use in inorganic or coordination chemistry is not as extensive.[34] The main reason for this is the difficulty of obtaining a reliable force field that accurately describes the bonding of metal ions. Another problem is the large number of different coordination geometries available to metal ions. Accelrys[35] has developed an extensive systematic force field (esff), which employs semi-empirical rules to translate atomic-based parameters, typically associated with a covalent force field. It takes into account the possible distortion of copper(II) from a regular octahedral geometry.[5] MM is a tool used to calculate the strain energy introduced into a ligand when coordinated to a metal ion.[36] This is one of the energy contributors to the total stability of the complex and hence its formation constant. Figure 7 shows possible structures for the different complexes of Cu(II) and L^1. The internal energies of these structures were calculated using the esff force field, and are reported in Table 2.

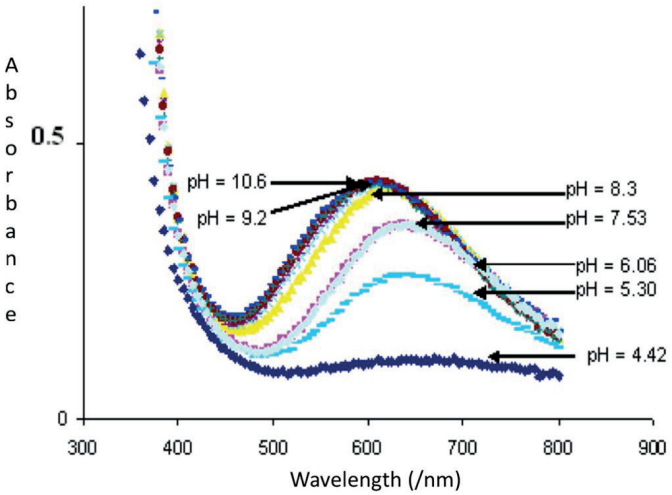

Figure 6: Absorption electronic spectra of Cu(II)-L^1 in solution as a function of pH.

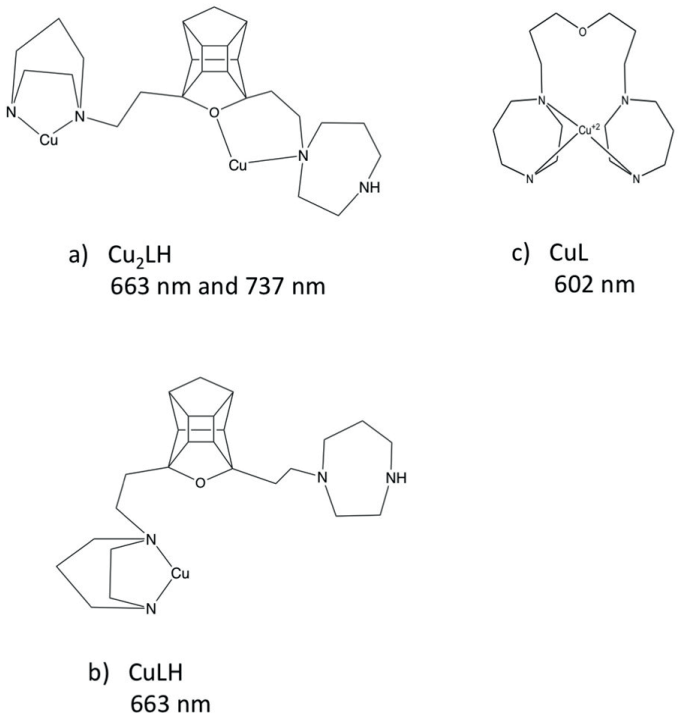

Figure 7: Proposed structures for the different Cu(II)-L^1 species. Coordinated water molecules are not shown.

Structures **a** and **b** (Figure 8) are two possible coordination geometries for the CuLH species, with the total potential energy of 113.15 kcal mol^{-1} and 163.54 kcal mol^{-1}, respectively. In structure **b**, one terminal amine and two tertiary amines bind to the metal ion, while the other terminal amine is protonated. In **a**, only one side of the ligand is involved in coordination. Comparing the change in internal energies given in Table 2, for structures **a** and **b**, structure **a** was chosen as the most likely representative structure for the CuLH species. This is consistent with the structure proposed from UV/Vis spectroscopy, where only two amine nitrogens were coordinated to the Cu(II). The large energy contribution to the total internal energy in structure **b** was the large bond deformation energy and the relatively high torsion energy, which is believed to be caused by the twisting of the ligand when trying to form this geometry.

The CuL species is believed to have more amine groups coordinated to the metal ion. This species is present in significant amounts at pH's > 8; therefore, we expect that all amines are either coordinated

Table 2: The bond, angle bending (angles), bond twisting (torsion), and total internal energy (kcal/mol) for the free ligand L^1H_4, CuL^1H, and CuL^1. (a)-(d) refer to the structures in Figure 8.

Species	Bond /kcal/mol	Angle /kcal/mol	Torsion /kcal/mol	Total energy /kcal/mol	Difference in internal energy between free ligand and complex /kcal/mol
Free ligand [LH_4]	4.29	42.36°	30.79	77.44	
[CuLH] (a)	15.20	62.25°	35.68	113.15	35.70
[CuLH] (b)	38.92	88.28°	36.33	163.54	86.09
[CuL] (c)	11.12	94.40°	42.35	147.90	70.45
[CuL] (d)	97.61	71.05°	43.04	211.73	134.28

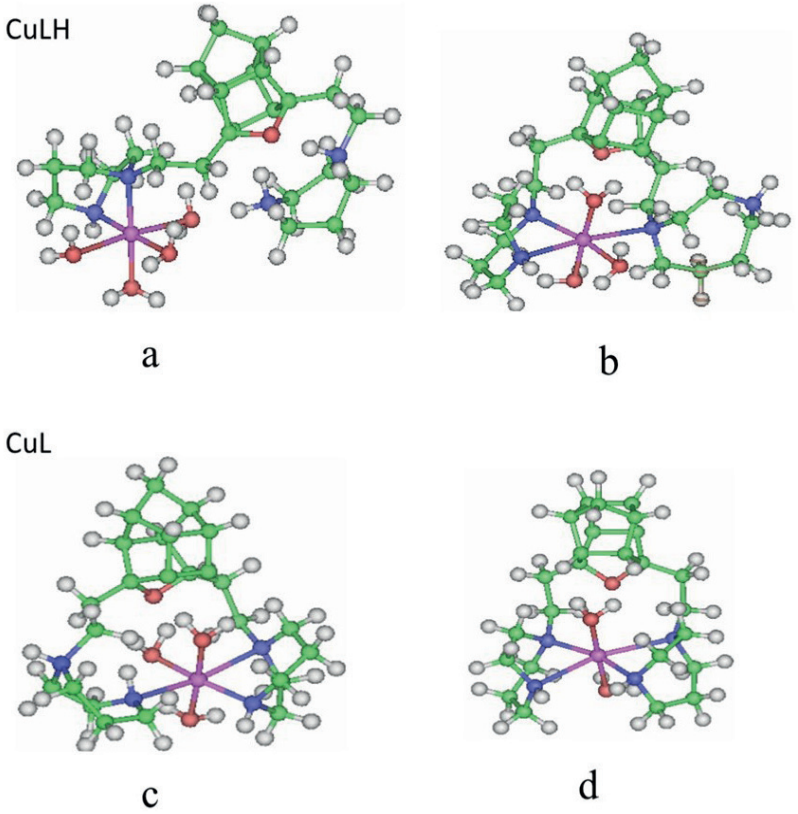

Figure 8: Possible conformations for the different species formed by the Cu(II)-L^1 calculated using Insight (II).

to the central metal ion or are deprotonated. The representative structures for the CuL species are shown in Figure 8(c,d) with their corresponding energies in Table 2. Structure **c** has an internal energy of 143 kcal mol^{-1}, and its coordination geometry is proposed to involve three amine groups coordinated to the Cu(II) ion. However, in the alternative structure, **d**, all four amines are coordinated to the metal ion, forming 2 highly strained, five-membered chelate rings and a ten-member ring (i.e. a (5, 10, 5)) system with an internal energy of 211.73 kcal mol^{-1}. Based on the MM calculations, it seems that L^1 is not a tetradentate ligand but behaves as a tridentate ligand. This structure is consistent with the structure of the CuL species determined from UV/Vis and NMR spectroscopy.

Blood-plasma Simulation Studies

The concentration of low molecular mass complexes in blood plasma can be increased by exogenous absorption or mobilisation from high molecular mass complexes. To test the ability of L^1 and L^2 to mobilise Cu(II) *in vivo*, the PMI was calculated using the ECCLES model of blood plasma.[37] A comparison of the stability constants alone is not enough because of the presence of other competing ligands and metal ions, which may be present at much higher concentrations. For example, the blood plasma concentration of Zn(II) is typically 10^{-3} mol dm^{-3}, while for Cu(II) it is only 10^{-16} mol dm^{-3}.[38,39] The total ligand concentration in the calculations was scanned from 1 to -10^{-10} mol dm^{-3}.

The PMI curves were calculated by incorporating the formation constants measured in this potentiometric study into the ECCLES model of blood plasma.[37] Figure 9a shows the PMI curves for Cu(II) together with two related ligands taken from the literature.[39] Although L^2 is slightly better than L^1 at mobilizing Cu(II), neither ligand is very effective. A ligand concentration of nearly 10^{-2} mol dm^{-3} is needed to increase the low molecular fraction of Cu(II) 10-fold. This can be compared with two related pentacyclo-undacane ligands, N,N'-bis[ethylenediamine]-4-[oxahexacyclododecane] (PCuA) and N, N'-bis [ethylenediamine]-4-[oxahexacyclododecane] (PCu.EN), which achieve the same result at 10^{-5} and 10^{-10} mol dm^{-3} respectively.[40] This means that any L^1 would not be able to release endogenous copper from its high molecular mass stores. Also, any copper complex of L^1 that is absorbed/administered would immediately release the copper to endogenous ligands.

Dermal Absorption (*in vitro*)

Low levels of bio-available copper in blood plasma have been associated with chronic inflammation and remission of symptoms seen with the administration of exogenous copper supplements.[12,41]

The use of copper bangles to suppress inflammation associated with RA has been known for a very long time.[12] Walker and Keats[12] have measured the dermal absorption from these bracelets and found it to be significant. The primary objective of *in vitro* dermal absorption studies is to evaluate the rate of dermal penetration or to predict the percentage of dermal absorption of an administered dose of a drug of interest.[42] *In vitro* dermal absorption studies provide key insights into the relationship between skin and drug formulation.[43] However, to date, there is little or no data involving a quantitative study of the bioavailability of copper using human skin *in vivo*.[44,45] The primary research methodology used in skin permeation studies is the Franz diffusion cell.[45] A modified Franz cell was used in this study, in which the donor and receiver phases were horizontal relative to each other. Also, an artificial membrane, Cerasome 9005, was used.

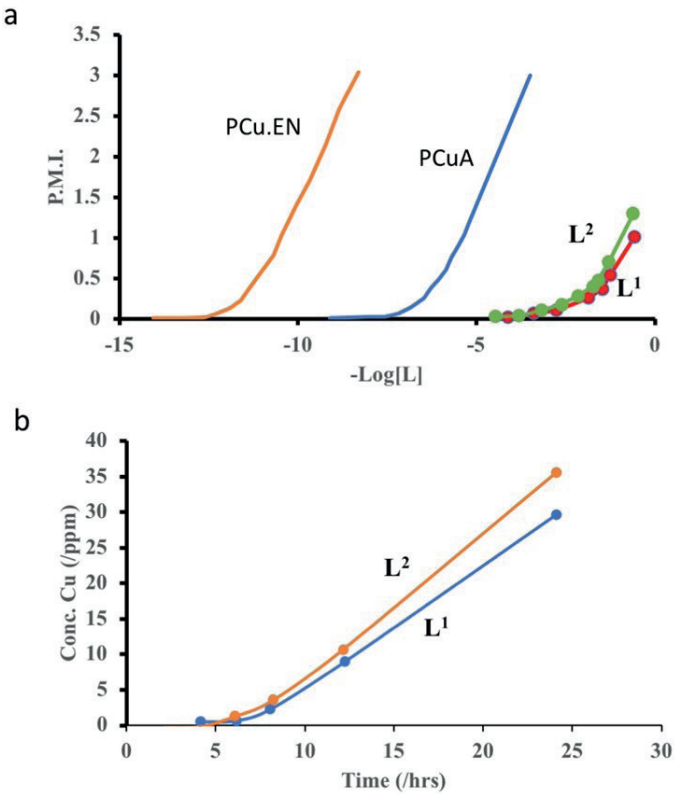

Figure 9: (**a**) PMI curve for L^1, L^2, and related ligand in blood plasma. PCUA=3.5-bis[ethanediamine]-4-[oxahexacyclododecane] and PCU.EN= N, N'-bis[ethylene diamine]-4-[oxahexacyclododecane]. (**b**) Diffusion of Cu(II)/L^2 and Cu(II)/L1 through a cerasome 9005 membrane.

The transdermal flux of CuL^1 and CuL^2, at pH 7.2, across the artificial membrane, Cerasome 9005, is shown in Figure 9b. The flux values and permeability coefficients are detailed in Table 3. Both complexes exhibited a slow diffusion phase during the first 8 hours, followed by a rapid increase in diffusion rate from 8 to 24 hours. This initial delay likely represents the establishment of equilibrium between the donor phase and the membrane. After this point, the rate of copper entry into the membrane equalled the rate entering the receiver phase.[43]

CuL^2 demonstrated greater permeability than CuL^1, likely due to the inverse relationship between molar mass and permeability.[46] For CuL^1, the permeability coefficient (log *K*p) was -5.30 ± 0.03, which is higher than that of [Cu(II)(gly-his-lys)] through stratum corneum (log *K*p = -7.17).[47] As expected, the diffusion through the stratum corneum is much slower as it is thicker and less permeable than Cerasome 9005. From the data in Table 3, it is clear that neither molar mass nor octanol/water partition coefficient is the principal factor affecting the permeability of copper complexes. Instead, the overall charge of the complex is important. The permeation coefficient of CuGly (K_p = 5.79 x 10^{-6} cm/s) is higher than that of CuL^1 (K_p = 5.06 x 10^{-6} cm/s) because the latter complex, in solution at pH 7.2, exists as a charged, CuLH species, while CuGly exists as the neutral, ML_2 species. The lowest flux was found for $[Cu(DTPA)]^{3-}$, which has the highest charge.

The results for L^1 and L^2 obtained using a Cerasome 9005 membrane can be compared to literature results obtained using isopropyl myristate as the artificial membrane (Table 3).[48–51] The tripeptides listed all have K_p values, some 2 orders of magnitude greater than L^1. This cannot be because of the molecular mass of L^1, since all the ligands listed have similar molecular masses. One of the reasons for adding pentacyclodecane to 1,4-diazepane was the idea that this would increase the lipophilicity and hence the permeability of the copper complex. This has not happened and may be related to the charge of the predominant copper complex present in the solution at 7.4. For L^1, 80% of the copper is present as the MLH species, which has a charge of +3. This can be compared to Sar-Leu-His, where all the copper is in the neutral MLH_{-2} species.

Table 3: Physicochemical parameters and Permeability coefficient, K_p, of copper (II) complexes of L^1, L^2, and related ligands taken from literature.[15, 47-50]

Complexes	Molecular Weight (MW) (mol/g)	K_p (mean ± SD) 10^{-6} s/cm	% Cu in main species	Log β	-Log K_{ow} [14]
CuL^1	416.51	5.06 ± 0.03	80 MLH	9.25	
CuL^2	163.14	5.63 ± 0.04	100 ML	7.60	3.49 ± 0.01
CuDTPA	414.77	2.17 ± 0.01	70 ML	8.69	3.62 ± 0.01
CuPrDH	314.79	2.28 ± 0.01	100 MLH_{-1}	5.00	3.45 ± 0.02
CuGly	138.566	5.79 ±0.04	100 ML_2	8.15	2.661 ± 0.003
CuH(555-N)	288.768	7.60 ± 0.03	100 MLH_{-1}	11.513	3.005 ± 0.007
CuGly-Leu-His	388.92	270.00 ± 0.03	100 MLH_{-2}	-2.24	3.25 ± 0.03
CuSar-Leu-His	402.74	226.67 ± 0.03	100 MLH_{-2}	-2.70	3.27 ± 0.03
CuGly-Phe-His	422.94	225.00 ± 0.03	100 MLH_{-2}	-1.03	3.10 ± 0.03
CuSar-Phe-His	436.96	253.33 ± 0.03	100 MLH_{-2}	-1.51	3.26 ± 0.04
CuSar-Lys-His	415.96	783.33 ± 0.01	98 MLH-1	05.41	2.05 ± 0.01
CuSar-His-Lys	434.96	816.67 ± 0.01	99 ML	09.44	3.02 ± 0.01
CuSar-Lys-Lys	407.97	1016.67 ± 0.01	25 ML 73 MLH-1	09.94	2.63 ± 0.01
CuSar-His-His	425.93	683.33 ± 0.01	77 ML 21 MLH-1	06.74	2.96 ± 0.01
CuSar-Gly-His	343.48	816.67 ± 0.01	96 MLH_{-2}	05.83	2.40 ± 0.01

CONCLUSION

The ligand, L^1, was synthesised and evaluated as a potential copper-based anti-inflammatory agent. Stability constants for both H^+ and Cu(II) complexes with ligands L^1 and L^2 were determined through potentiometric studies at 25 °C and 0.15 mol dm^{-3} NaCl over a pH range of 2–11. The protonation behaviour of L^1 showed two secondary amines with moderate to high basicity, consistent with other tetra-amine ligands. NMR spectroscopy data gave pKa values of 10.1 and 9.0 for the terminal amines of L^1, which accorded with the potentiometric results. UV/Vis spectroscopy suggested that L^1 coordinates with Cu(II) in a distorted tetragonal arrangement. This conclusion was supported by molecular modelling.

Our primary goal was to develop a ligand that could enhance the bioavailability of copper in blood plasma, either by mobilising copper from endogenous stores or through transdermal absorption. However, plasma mobilisation studies showed that both L^1 and L^2 had limited ability to increase copper availability *in vivo*. Dermal permeability studies, using a Cerasome 9005 membrane as a skin model, revealed that the permeability of the Cu-L^1 complex is comparable to that of $CuGly_2$, indicating that L^1 is unlikely to significantly enhance copper absorption through the skin. A previous study, using the amide analogue of L^1, found the copper binding of the ligand to be too weak for effective copper chelation therapy. [6] Converting the amide to an amine in L^1 did improve the copper chelation, but not sufficiently for use as a copper therapeutic. Therefore, L^1 does not appear to be a suitable candidate for a copper-based anti-inflammatory drug for RA treatment.

SUPPLEMENTARY INFORMATION

Original NMR spectra are given as supplementary information

ACKNOWLEDGMENTS

This work is based on the research supported in part by the National Research Foundation of South Africa (Grant Numbers 93450 and 85466) and the University of Cape Town Research Committee. The Centre for HighPerformance Computing (CHPC), South Africa, provided computational resources for this research project.

CREDIT AUTHORSHIP CONTRIBUTION STATEMENT

Kagiso Mokalane submitted sections of this work to the University of Cape Town as partial fulfilment of the thesis requirements for the MSc degree. Graham Jackson conceptualised and funded the project, supervised, interpreted the results and wrote the final draft. Ahmed Hammouda and Fatin Elmagbari supervised, interpreted and wrote the first draft of the paper. The ligand was synthesised by Oluseye K. Onajole under the supervision of Hendrik G. Kruger. All authors contributed to the final version of the paper.

DECLARATION OF COMPETING INTEREST

The authors declare that they have no known competing financial interests or personal relationships that could have appeared to influence the work reported in this paper.

DECLARATION OF GENERATIVE AI AND AI-ASSISTED TECHNOLOGIES

AI was not used in the preparation of the manuscript or the interpretation of the data.

ORCID ID

Graham Jackson: https://orcid.org/0000-0002-4243-5470
Hendrik G. Kruger: https://orcid.org/0000-0003-0606-2053
Oluseye K. Onajole: https://orcid.org/0000-0002-4485-9648
Ahmed N. Hammouda: https://orcid.org/0000-0002-7816-0261
Fatin M. Elmagbari: https://orcid.org/0000-0002-0019-9211

REFERENCES

1. Burmester GR, Pope JE. Novel treatment strategies in rheumatoid arthritis. Lancet. 2017;389(10086):2338–2348. https://doi.org/10.1016/S0140-6736(17)31491-5.
2. Odisitse S, Jackson GE. In vitro and in vivo studies of the dermally absorbed Cu(II) complexes of N5O2 donor ligands – Potential anti-inflammatory drugs. Inorg Chim Acta. 2009;362(1):125–135. https://doi.org/10.1016/j.ica.2008.03.092.
3. Weyand CM. New insights into the pathogenesis of rheumatoid arthritis. Rheumatology (Oxford). 2000;39(1) suppl_1:3–8. https://doi.org/10.1093/oxfordjournals.rheumatology.a031491.
4. Choy E. Understanding the dynamics: pathways involved in the pathogenesis of rheumatoid arthritis. Rheumatology (Oxford). 2012;51(5) suppl 5:v3–v11. https://doi.org/10.1093/rheumatology/kes113.
5. Odisitse S, Jackson GE, Govender T, Kruger HG, Singh A. Chemical speciation of copper(II) diaminediamide derivative of pentacycloundecane—a potential anti-inflammatory agent. Dalton Trans. 2007;(11):1140–1149. https://doi.org/10.1039/B614878F.
6. Odisitse S, Jackson GE. In vitro and in vivo studies of N,N'-bis[2(2-pyridyl)-methyl]pyridine-2,6-dicarboxamide–copper(II) and rheumatoid arthritis. Polyhedron. 2008;27(1):453–464. https://doi.org/10.1016/j.poly.2007.09.032.
7. Jackson GE, Mkhonta-Gama L, Voyé A, Kelly M. Design of copper-based anti-inflammatory drugs. J Inorg Biochem. 2000;79(1-4):147–152. https://doi.org/10.1016/S0162-0134(99)00171-3.
8. Zvimba JN, Jackson GE. Thermodynamic and spectroscopic study of the interaction of Cu(II), Ni(II), Zn(II) and Ca(II) ions with 2-amino-N-(2-oxo-2-(2-(pyridin-2-yl)ethyl amino)ethyl)acetamide, a pseudo-mimic of human serum albumin. Polyhedron. 2007;26(12):2395–2404. https://doi.org/10.1016/j.poly.2006.11.053.
9. Sanz I, Alboukrek D. Rheamatoid Arthritis. Fischbach M, editor. New York, Edinburg: Churchill Livingstone; 1991.
10. Sorenson JR. Evaluation of copper complexes as potential anti-arthritic drugs. J Pharm Pharmacol. 1977;29:450–452. https://doi.org/10.1111/j.2042-7158.1977.tb11367.x
11. Weder JE, Dillon CT, Hambley TW, Kennedy BJ, Lay PA, Biffin JR, Regtop HL, Davies NM. Copper complexes of non-steroidal anti-inflammatory drugs: an opportunity yet to be realized. Coord Chem Rev. 2002;232(1–2):95–126. https://doi.org/10.1016/S0010-8545(02)00086-3.
12. Walker WR, Keats DM. An investigation of the therapeutic value of the 'copper bracelet'-dermal assimilation of copper in arthritic/rheumatoid conditions. Agents Actions. 1976;6(4):454–459.
13. Korinth G, Schaller KH, Drexler H. Is the permeability coefficient Kp a reliable tool in percutaneous absorption studies? Arch Toxicol. 2005;79(3):155–159. https://doi.org/10.1007/s00204-004-0618-4.
14. Mazurowska L, Nowak-Buciak K, Mojski M. ESI-MS method for in vitro investigation of skin penetration by copper-amino acid complexes: from an emulsion through a model membrane. Anal Bioanal Chem. 2007;388(5-6):1157–1163. https://doi.org/10.1007/s00216-007-1345-5.
15. Péhourcq F, Matoga M, Jarry C, Bannwarth B. Study of the lipophilicity of arylpropionic non-steroidal anti-inflammatory drugs. A comparison between lc retention data on a polymer-based column and octanol-water partition coefficients. J Liq Chromatogr Relat Technol. 2001;24(14):2177–2186. https://doi.org/10.1081/JLC-100104900.
16. Odisitse S, Jackson GE. Potentiometric and blood plasma simulation studies of nickel(ii) complexes of poly(amino)amido pentadentate ligands: computer aided metal-based drug design. Bioinorg Chem Appl. 2014;2014:863612. https://doi.org/10.1155/2014/863612.
17. Morgan E. Vogel's textbook of practical organic chemistry. 5th edn. Harlow: Longman Scientific & Technical; 1990. https://doi.org/10.1016/0160-9327(90)90017-L.
18. Murray K, May PM. ESTA: Equilibrium Simulation for Titration Analysis. University of Wales Institute of Science and Technology (UWIST) Department of Applied Chemistry, 1984.
19. May PM, Linder PW, Williams DR. Computer simulation of metal-ion equilibria in biofluids: models for the low-molecular-weight complex distribution of calcium(II), magnesium(II), manganese(II), iron(III), copper(II), zinc(II), and lead(II) ions in human blood plasma. J Chem Soc, Dalton Trans. 1977;2(6):588. https://doi.org/10.1039/dt9770000588.

20. Starmark JE, Hellström PH, Agren H. When disease insight is halting. II. The neurobiological underpinnings. Lakartidningen. 2000;97:328–331.
21. Hancock RD. Polar and steric effects in the stability of silver complexes of primary amines. J Chem Soc, Dalton Trans. 1980;416(3):416. https://doi.org/10.1039/dt9800000416.
22. Machida R, Kimura E, Kodama M. Dioxygen uptake by cobalt(II) complexes of macrocyclic polyamines. Effects of chelate ring size and substituents. Inorg Chem. 1983;22(14):2055–2061. https://doi.org/10.1021/ic00156a023.
23. Dhont KI, Herman GG, Fabretti AC, Lippens W, Goeminne AM. Protonation and metal-ion complexation in aqueous solution by pyridine-containing hexaaza macrocycles. J Chem Soc, Dalton Trans. 1996;1753(8):1753. https://doi.org/10.1039/dt9960001753.
24. Chellquist EM, Searle R. An LC method for measuring complex formation equilibria by competitive chelation. J Pharm Biomed Anal. 1993;11(10):985–992. https://doi.org/10.1016/0731-7085(93)80059-A.
25. Kroneck PM, Vortisch V, Hemmerich P. Model studies on the coordination of copper in biological systems. The deprotonated peptide nitrogen as a potential binding site for copper(II). Eur J Biochem. 1980;109(2):603–612. https://doi.org/10.1111/j.1432-1033.1980.tb04833.x.
26. Pagano JM, Goldberg DE, Fernelius WC. A thermodynamic study of homopiperazine, piperazine and n-(2-aminoethyl)-piperazine and their complexes with copper(II) ion. J Phys Chem. 1961;65(6):1062–1064. https://doi.org/10.1021/j100824a513.
27. Laussac JP, Haran R, Sarkar BN. N.M.R. and E.P.R. investigation of the interaction of copper(II) and glycyl-l-histidyl-l-lysine, a growth-modulating tripeptide from plasma. Biochem J. 1983;209(2):533–539. https://doi.org/10.1042/bj2090533.
28. Epperson JD, Ming LJ. Proton NMR studies of Co(II) complexes of the peptide antibiotic bacitracin and analogues: insight into structure-activity relationship. Biochemistry. 2000;39(14):4037–4045. https://doi.org/10.1021/bi991997p.
29. Lever ABP. Inorganic Electron Spectroscopy. Studies in Physical & Theoretical Chemistry. Amsterdam: Elsevier Science Publishers B.V.; 1984.
30. Jaffe HH. O. M. Theory & Applications of Ultraviolet Spectroscopy. New York, London, New York: John Willey & Sons; 1962.
31. Billo EJ. Copper(II) chromosomes and the rule of average environment. Inorg Nucl Chem Lett. 1974;10(8):613–617. https://doi.org/10.1016/0020-1650(74)80002-4.
32. Lever ABP. Inorganic electronic Spectroscopy. Amsterdam: Elsevier; 1968.
33. Jackson GE, Linder PW, Voye' A. A potentiometric and spectroscopic study of copper(II) diamidodiamino complexes. J Chem Soc, Dalton Trans. 1996;4605(24):4605–4612. https://doi.org/10.1039/DT9960004605.
34. Sun X, Wuest M, Kovacs Z, Sherry DA, Motekaitis R, Wang Z, Martell AE, Welch MJ, Anderson CJ. In vivo behavior of copper-64-labeled methanephosphonate tetraaza macrocyclic ligands. J Biol Inorg Chem. 2003;8(1):217–225. https://doi.org/10.1007/s00775-002-0408-5.
35. Insight II, version 2005, San Diego: Accelrys Inc., http://www.accelrys.com
36. Mannfors B, Pietilä L-O, Palmö K, Sundius T, Krimm S. Molecular mechanics potential energy functions from vibrational spectroscopy and quantum chemistry. J Mol Struct. 1997;408–409:63–69. https://doi.org/10.1016/S0022-2860(96)09454-9.
37. Jackson GE, May PM, Williams DR. Metal-ligand complexes involved in rheumatoid arthritis—VI. J Inorg Nucl Chem. 1978;40:1227–1234. https://doi.org/10.1016/0022-1902(78)80544-2.
38. William RD. The Metals of Life. London: Van Norstrand Reinhold; 1971.
39. John RJ. The Anti-Inflammatory Activities of Copper Complexes. In: Sigel H, editor. Metal Ions in Biological Systems: Volume 14: Inorganic Drugs in Deficiency and Disease (1st ed.). CRC Press. 48 p. https://doi.org/10.1201/9781003418061.
40. Odisitse S, Jackson GE. In Vivo bio-distribution study of ^{64}Cu(II)-labelled copper (II) complexes of peptides mimics in balb/c mice-development of copper based anti-inflammatory agents. MOJ Biorg Org Chem. 2017;1(5):153–157. https://doi.org/10.15406/mojboc.2017.01.00029.
41. Walker WR. The Results of a Copper Bracelet Clinical Trial and Subsequent Studies. In: Sorenson JRJ, editor. Inflammatory Diseases and Copper. Experimental Biology and Medicine, vol 2. Totowa: Humana Press; 1982. pp 469–482. https://doi.org/10.1007/978-1-4612-5829-2_42.
42. Ng S-F, Rouse J, Sanderson D, Eccleston G. A comparative study of transmembrane diffusion and permeation of ibuprofen across synthetic membranes using Franz diffusion cells. Pharmaceutics. 2010;2(2):209–223. https://doi.org/10.3390/pharmaceutics2020209.
43. Ng S-F, Rouse JJ, Sanderson FD, Meidan V, Eccleston GM. Validation of a static Franz diffusion cell system for in vitro permeation studies. AAPS PharmSciTech. 2010;11(3):1432–1441. https://doi.org/10.1208/s12249-010-9522-9.
44. Bosman I. Standardization procedure for the in vitro skin permeation of anticholinergics. Int J Pharm. 1998;169(1):65–73. https://doi.org/10.1016/S0378-5173(98)00106-9.
45. Mazurowska L, Mojski M. Biological activities of selected peptides: skin penetration ability of copper complexes with peptides. J Cosmet Sci. 2008;59:59–69.
46. Umba-Tsumbu E, Hammouda AN, Jackson GE. Evaluation of membrane permeability of copper-based drugs. Inorganics (Basel). 2023;11(5):179. https://doi.org/10.3390/inorganics11050179.
47. Hostynek JJ, Dreher F, Maibach HI. Human skin penetration of a copper tripeptide in vitro as a function of skin layer. Inflamm Res. 2011;60(1):79–86. https://doi.org/10.1007/s00011-010-0238-9.
48. Jackson GE, Hammouda AN, Elmagbari FM, Bonomo RP. In vitro studies of dermally absorbed Cu(II) tripeptide complexes as potential anti-inflammatory drugs. Polyhedron. 2017;123:23–32. https://doi.org/10.1016/j.poly.2016.10.048.
49. Vicatos GM, Jackson GE, Hammouda AN, Bonomo RP, Valora G. Potentiometric and spectroscopic studies of the complex formation between copper(II) and Gly-Leu-Phe or Sar-Leu-Phe tripeptides. Polyhedron. 2019;170:553–563. https://doi.org/10.1016/j.poly.2019.06.011.
50. Alsaqir AA, Elmagbari FM, Vicatos GM, Hammouda AN, Jackson GE, Ben Amer YO, El-Ferjani RM. *In silico* studies, partition coefficients and tissue permeability of Cu (II) tripeptide species as potential anti-inflammatory drugs. The Libyan Conference on Chemistry and Its Applications (LCCA 2021), Benghazi, Libya, 15–16 December 2021. pp. 62–69.
51. Hammouda AN, Elmagbari FM, Jackson GE, Vicatos GM, Bonomo RP, Valora G. Stability, structure, and permeability studies of copper tripeptide species in aqueous solution. Aust J Chem. 2021;74(8):613–622. https://doi.org/10.1071/CH21040.